



Automated volumetry of core and peel intrapulmonary vasculature on computed tomography angiography for non-invasive estimation of hemodynamics in patients with pulmonary hypertension (2022 updated hemodynamic definition)

Claudius Melzig^{1,2,^}, Oliver Weinheimer^{1,2}, Benjamin Egenlauf^{2,3}, Thuy D. Do^{1,2}, Mark O. Wielpütz^{1,2}, Ekkehard Grünig^{2,3}, Hans-Ulrich Kauczor^{1,2}, Claus Peter Heussel^{2,4}, Fabian Rengier^{1,2}

¹Clinic for Diagnostic and Interventional Radiology, Heidelberg University Hospital, Heidelberg, Germany; ²Translational Lung Research Center Heidelberg (TLRC), Member of the German Center for Lung Research (DZL), University of Heidelberg, Heidelberg, Germany; ³Centre for Pulmonary Hypertension, Thoraxklinik at Heidelberg University Hospital, Heidelberg, Germany; ⁴Department of Radiology, Thoraxklinik at Heidelberg University Hospital, Heidelberg, Germany

Contributions: (I) Conception and design: C Melzig, F Rengier, O Weinheimer; (II) Administrative support: E Grünig, HU Kauczor, CP Heussel, MO Wielpütz; (III) Provision of study materials or patients: E Grünig, B Egenlauf, CP Heussel, O Weinheimer; (IV) Collection and assembly of data: C Melzig, TD Do, B Egenlauf, O Weinheimer, F Rengier; (V) Data analysis and interpretation: C Melzig, O Weinheimer, F Rengier, MO Wielpütz; (VI) Manuscript writing: All authors; (VII) Final approval of manuscript: All authors.

Correspondence to: Claudius Melzig, MD. Clinic for Diagnostic and Interventional Radiology, Heidelberg University Hospital, Im Neuenheimer Feld 420, 69120 Heidelberg, Germany; Translational Lung Research Center Heidelberg (TLRC), Member of the German Center for Lung Research (DZL), University of Heidelberg, Heidelberg, Germany. Email: c.melzig@icloud.com.

Background: Computed tomography pulmonary angiography (CTPA) is frequently performed in patients with pulmonary hypertension (PH) and may aid non-invasive estimation of pulmonary hemodynamics. We, therefore, investigated automated volumetry of intrapulmonary vasculature on CTPA, separated into core and peel fractions of the lung volume and its potential to differentially reflect pulmonary hemodynamics in patients with pre- and postcapillary PH.

Methods: A retrospective case-control study of 72 consecutive patients with PH according to the 2022 joint guidelines of the European Society of Cardiology and the European Respiratory Society who underwent right heart catheterization (RHC) and CTPA within 7 days between August 2013 and February 2016 at Thoraxklinik at Heidelberg University Hospital (Heidelberg, Germany) was conducted. Vessel segmentation was performed using the in-house software YACTA. Vascular volumes in different core and peel fractions of the lung were corrected for body surface area. Spearman correlation coefficients with mean pulmonary arterial pressure (mPAP), pulmonary arterial wedge pressure (PAWP) and pulmonary vascular resistance (PVR) were calculated, and a linear regression analysis was done to account for potential confounders.

Results: Median age of the study sample was 71.5 years [interquartile range (IQR), 60.0–77.0 years], 48 (66.67%) were female. Median mPAP was 35.5 mmHg (IQR, 27.0–47.2 mmHg). Postcapillary PH was present in 24/72 (33.3%) patients and precapillary PH in 48/72 (66.7%) patients. Moderate to strong correlations between core intrapulmonary vessel volumes and mPAP were observed in postcapillary PH patients with a maximum at 50% core lung volume ($r=0.71$, $P<0.001$). No significant influence of age or sex on this relationship was identified. Correlation with RHC measurements was weak or negligible in patients with precapillary PH.

Conclusions: Automated volumetry of vessels in the core lung strongly correlated with mPAP in patients with postcapillary PH and has potential for non-invasive assessment of postcapillary PH in patients undergoing CTPA.

[^] ORCID: 0000-0003-1077-4977.

Keywords: Pulmonary hypertension (PH); left heart disease; computed tomography pulmonary angiography (CTPA); pulmonary vasculature; automated segmentation

Submitted Jun 26, 2024. Accepted for publication Aug 18, 2024. Published online Dec 19, 2024.

doi: 10.21037/cdt-24-293

View this article at: <https://dx.doi.org/10.21037/cdt-24-293>

Introduction

Background

Pulmonary hypertension (PH) is defined by a pathological increase in mean pulmonary arterial pressure (mPAP) (1,2). It can occur as an isolated condition but most commonly represents a complication of a pre-existing condition, such as heart or lung disease. The clinical classification of PH mirrors this, grouping PH forms based on hemodynamic characteristics and treatment strategies (1). The diagnosis of PH requires invasive measurement of mPAP via right heart catheterization (RHC). Recently, a revised hemodynamic definition of PH, lowering the mPAP threshold for the diagnosis of PH from ≥ 25 to >20 mmHg, had been proposed during the 6th World Symposium on Pulmonary Hypertension in 2018 (3) and was subsequently adopted

by the 2022 joint guidelines by the European Society of Cardiology (ESC) and the European Respiratory Society (ERS) (1). Additionally, measurements of pulmonary arterial wedge pressure (PAWP) are required to differentiate postcapillary types of PH (PAWP >15 mmHg) from precapillary PH and pulmonary vascular resistance (PVR) is needed to quantify a precapillary component of PH. PH due to left heart disease is a form of postcapillary PH and the most frequent type of PH (4). Its treatment differs from precapillary types of PH and focusses on the underlying heart disease (1).

Rationale and knowledge gap

PH is associated with remodelling of the pulmonary vasculature, resulting in pruning of the small pulmonary vessels and increased pulmonary arterial pressure (5,6). Consecutive increases in diameter and volume of the extrapulmonary main pulmonary arteries in patients with PH have been repeatedly demonstrated (7-12). Computed tomography pulmonary angiography (CTPA) is frequently performed in patients with PH to rule out pulmonary embolism and to assess the lung parenchyma (1). Recent studies have suggested potential use of automated segmentation of central pulmonary arteries or cardiac chambers on CTPA in patients with confirmed or suspected PH to improve patient selection for invasive hemodynamic testing (12-16). However, only a few studies have investigated segmentation of the intrapulmonary vasculature and mainly focused on the most peripheral vessels (10,17-23). Furthermore, few data have been published on intrapulmonary vascular volume in patients with PH according to the updated hemodynamic definitions per the 2022 updated ESC/ERS guidelines.

Objective

For the present study we hypothesized that intrapulmonary vascular volume separated into core and peel fractions of the lung volume may differentially reflect pulmonary

Highlight box

Key findings

- Automated volumetry of core and peel intrapulmonary vessels based on computed tomography is feasible.
- Vessel volume in the core lung strongly correlates with mean pulmonary arterial pressure (mPAP) in patients with postcapillary pulmonary hypertension (PH).

What is known and what is new?

- The main pulmonary arteries are known to be dilated in patients with PH and a reduction in small peripheral pulmonary vessels has been demonstrated in patients with various forms of PH.
- Systematic analysis of intrapulmonary vessel volumes in various core and peel fractions of the lung, which had not been previously conducted, identified a strong correlation between core intrapulmonary vessel volumes and mPAP in patients with postcapillary PH with a maximum at 50% core lung volume.

What is the implication, and what should change now?

- The technique might assist in non-invasive hemodynamic evaluation in patients with postcapillary PH and may have further potential for treatment monitoring.
- The technique should be evaluated further in larger, prospective studies to validate its use for non-invasive evaluation of patients with postcapillary PH.

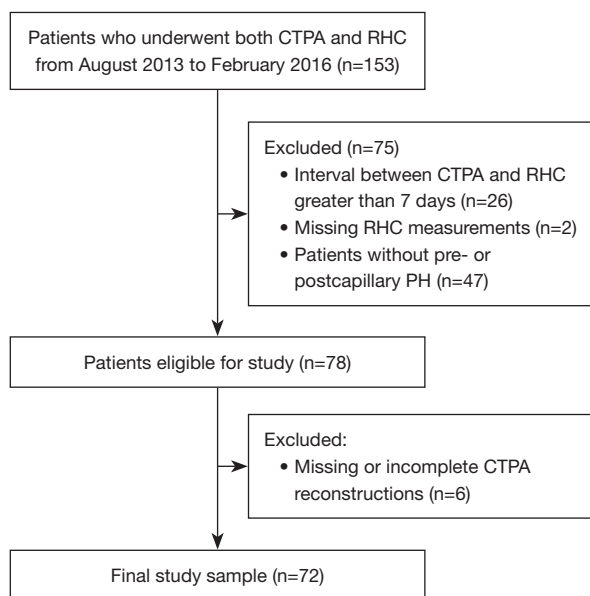


Figure 1 Flow diagram illustrating study inclusion. CTPA, computed tomography pulmonary angiography; RHC, right heart catheter; PH, pulmonary hypertension.

hemodynamics in PH. Therefore, we investigated automated volumetry of intrapulmonary vasculature in core and peel fractions of the lung volume for its potential for non-invasive estimation of pulmonary hemodynamics in patients diagnosed with PH according to the 2022 ESC/ERS guidelines. We present this article in accordance with the STROBE reporting checklist (available at <https://cdt.amegroups.com/article/view/10.21037/cdt-24-293/rc>).

Methods

Patients

The study was conducted in accordance with the Declaration of Helsinki (as revised in 2013). The study was approved by the ethics committee of the medical faculty of Heidelberg University (No. S-592/2016) and individual consent for this retrospective analysis was waived. Records of all patients within a 30-month period from August 2013 to February 2016 undergoing both RHC and CTPA at Thoraxklinik at Heidelberg University Hospital (Heidelberg, Germany) were reviewed. Patients with an interval between CTPA and RHC of no more than 7 days and with precapillary or postcapillary (isolated postcapillary and combined pre- and postcapillary) PH, as defined by the 2022 ESC/ERS guidelines, were included in the study.

Patients had to be excluded in case of missing RHC data or missing slices from the reconstructed CTPA images in the institutional PACS, prohibiting complete automated segmentation of the lung vasculature. Detailed inclusion and exclusion criteria are summarized in *Figure 1*. Patient characteristics (sex, size, age) were extracted from the records, body surface area (BSA) was calculated according to the formula by Du Bois and Du Bois (24).

CTPA acquisition

CTPA was acquired using a 64-slice scanner (Somatom Definition AS 64, Siemens Healthineers, Erlangen, Germany). Patients were examined in supine position during inspiratory breath-hold without electrocardiogram (ECG) gating. Bolus tracking in the main pulmonary artery was utilised to trigger injection of 50 mL of contrast medium [Iopromide (Ultravist 300, Bayer AG, Berlin, Germany)] at a rate of 3–5 mL/s followed by a saline chaser bolus of 50 mL at an identical rate. A reference tube current of 100 mAs and a tube potential of 120 kV_p were set for automated tube voltage selection and tube current modulation. Reconstruction of CTPA images was done using an I40f kernel, sinogram-affirmed iterative reconstruction (SAFIRE, Siemens Healthineers) with strength level 3, a slice thickness of 1 mm, and slice increments of 0.7 mm.

Image analysis

Fully automatic image analysis was performed using the software YACTA (“yet another CT analyser”; version 2.9.1.10) as employed in previous studies (25–28). Automated segmentations were reviewed and validated by a board-certified radiologist (C.M.) with 8 years of experience in cardiovascular imaging. Airway segmentation was performed with a self-adapting iterative region growing algorithm. Central airways and lobar bronchi were labelled by an anatomical knowledge-based algorithm. The lung parenchyma segmentation delivers masks of the right and left lung as well as for the lobes (*Figure 2*). Then an initial vessel segmentation is performed by using a threshold-based algorithm with an adjusted threshold for each computed tomography (CT). Vessels that are not completely within the lung segmentation on the transverse cross-sectional images are excluded—this leads to the exclusion of the large vessels in the hilar region, see arrows in *Figure 2E*. Three-dimensionally (3D) connected vessel objects are generated from the initial vessel segmentation, just vessel objects

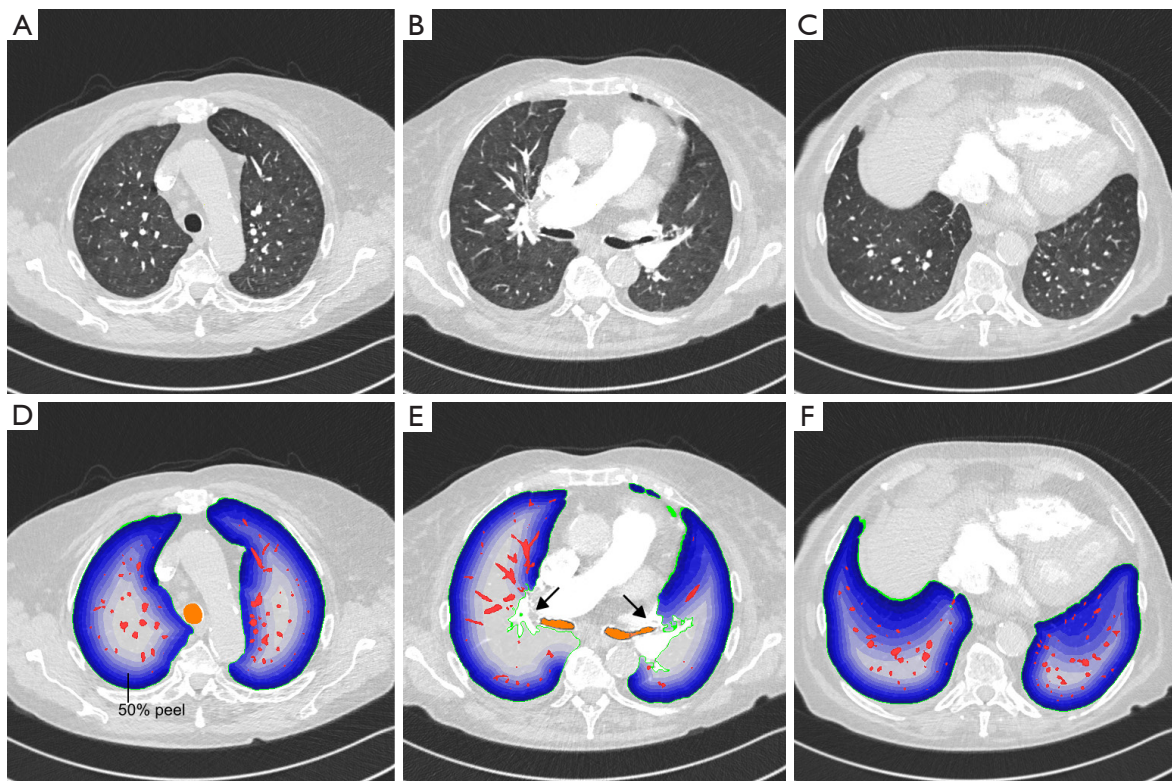


Figure 2 Illustration of core-peel division of the lung and vessel segmentation. Original transversal computed tomography slices from the upper (A) middle (B) and lower (C) lung region. (D-F) Green contour indicates the lung border and bronchi are displayed in orange (D,E). The different core-peel divisions are shown as blue gradations: dark blue 10% peel, to very light blue 100% peel. The segmented 3D connected vessels are displayed in red. In (D) the 50% core-peel division is shown, arrows in (E) point to the hilar lung region which is handled as the root of the core lung region, note that large vessels are excluded.

larger than 100 mm^3 are retained. The applied workflow is shown in more detail in (25). For this project the lung segmentation was divided in a core and peel region, whereby the region, where the main bronchi and the large vessels enter the lung parenchyma, was defined as the root of the lung core (Figure 2E). The core-peel division of the lungs was performed in 10% increments (Figure 2D-2F). To achieve this, the lung border voxels were defined as first peel layer. This layer was dilated until the desired percentage for core-peel division was reached. Intrapulmonary vessel volume was automatically calculated for the whole lung and within varying peel fractions of the total lung volume. Vessel volumes within lung core fractions were then calculated by subtraction of the peel volumes from the total vessel volume for every patient. Resulting vessel volumes were then corrected for the respective patient's BSA. For further analysis, total intrapulmonary vessel volume and the 20%, 50% and 80% core and peel lung volume fractions were selected.

RHC

RHCs were performed according to guidelines by an interventional cardiologist (E.G.) and an interventional pulmonologist (B.E.), both with more than 9 years of experience in RHC (1). In brief, a 7-French pulmonary artery catheter was inserted via the right internal jugular vein, and pulmonary arterial pressure measurements were performed after zero levelling. The RHC measurements mPAP, PVR, and PAWP were extracted from the electronic medical record.

Definition of PH

Patients were classified in terms of presence or absence of pre- or postcapillary PH based on RHC measurements according to the updated hemodynamic definition included in the 2022 ESC/ERS guidelines for the diagnosis and

Table 1 Patient characteristics of the study sample

Characteristics	All patients (n=72)	Postcapillary PH (n=24)	Precapillary PH (n=48)	P value
Age (years)	71.5 (60.0–77.0)	75.0 (69.5–77.2)	68.0 (60.0–75.2)	0.03
Female	48 (66.67)	19 (79.17)	29 (60.42)	0.18
Height (m)	1.65±0.0717	1.63±0.0753	1.66±0.0687	0.13
Weight (kg)	74.38±16.46	77.97±15.62	72.58±16.72	0.18
BSA (m ²)	1.81±0.197	1.83±0.188	1.80±0.202	0.47
CT-RHC interval (days)	1.0 (0.0–1.0)	1.0 (0.8–1.0)	1.0 (0.0–1.0)	0.99
Mean PAP (mmHg)	35.5 (27.0–47.2)	40.5 (31.0–48.0)	32.0 (27.0–45.2)	0.11
Systolic PAP (mmHg)	53.0 (42.0–73.0)	60.0 (46.8–76.0)	52.0 (41.0–72.0)	0.20
Diastolic PAP (mmHg)	23.5 (18.0–29.2)	27.5 (22.2–31.0)	22.5 (17.8–28.2)	0.06
PAWP (mmHg)	12.0 (9.0–18.2)	22.0 (18.8–26.0)	10.0 (7.0–12.0)	<0.001
PVR (Wood units)	3.8 (2.6–7.6)	2.7 (2.3–4.7)	4.8 (3.1–8.5)	0.005
CO (L/min)	4.7 (3.9–5.8)	4.4 (4.0–5.3)	4.8 (3.9–5.8)	0.53

Values are presented as mean ± SD, number of patients (percentage), or median (interquartile range), as appropriate according to Shapiro-Wilk test of distribution. SD, standard deviation; BSA, body surface area; CO, cardiac output; CT, computed tomography; PAP, pulmonary arterial pressure; PAWP, pulmonary arterial wedge pressure; PH, pulmonary hypertension; PVR, pulmonary vascular resistance; RHC, right heart catheterization.

treatment of PH (1). Per these guidelines, diagnosis of postcapillary PH requires an elevated mPAP >20 mmHg and an elevated PAWP >15 mmHg in combination with a PVR of ≤2 Wood units (isolated postcapillary PH) or >2 Wood units (combined pre- and postcapillary PH). Precapillary PH is defined by an elevated mPAP greater than 20 mmHg and a PVR >2 Wood units combined with a normal PAWP ≤15 mmHg, according to the current guidelines. Further classification into different PH groups was based on the diagnosis in patients' records.

Statistical analysis

Shapiro-Wilk test and Q-Q-plots were employed to test for normal distribution. Normally distributed continuous data were expressed as mean ± standard deviation, non-normally distributed data were expressed as median and interquartile range (IQR) and categorical data were expressed as numbers and percentages. Spearman's correlation coefficients were calculated between intrapulmonary vascular volumes and RHC measurements and absolute values interpreted as follows (29): <0.1–<0.2 very weak/negligible, ≥0.2–<0.4 weak, ≥0.4–<0.7 moderate, ≥0.7–<0.9 strong, ≥0.9–1.0 very strong. A bootstrapping method was used to calculate 95%

confidence intervals (CIs) for the most significant correlations using 1,000 iterations in each case. Multivariable linear regression analyses were conducted to estimate the effect of cardiac output (CO) and PH group and intrapulmonary vascular volume and to assess the influence of potential confounders on estimation of mPAP. P values <0.05 for two-sided tests were considered statistically significant. All statistical analyses were performed using R Version 4.0.2 (R Foundation for Statistical Computing).

Results

Study cohort

The final study sample consisted of 72 patients (*Figure 1, Table 1*). Median mPAP in the study sample was 35.5 mmHg (IQR, 27.0–47.2 mmHg), with a minimum mPAP of 21 mmHg and a maximum mPAP of 79 mmHg. Of all included patients, 24/72 (33.3%) had postcapillary PH according to the updated 2022 hemodynamic definition. Of these, 5/24 (20.8%) had isolated postcapillary PH and 19/24 (79.2%) had combined pre- and postcapillary PH. Precapillary PH was present in 48/72 patients (66.7%). Of these patients, 20/48 (41.7%) were classified as group 1 PH, 15/48 (31.3%) as group 4 PH and 5/48 (10.4%) as group 3 PH according

Table 2 Intrapulmonary vessel volumes within different core and peel fractions of the lung volume

Lung volume fraction	All patients (mL/m ²)	Precapillary PH (mL/m ²)	Postcapillary PH (mL/m ²)	P value
Whole lung	74.1 (64.8–91.9)	75.0 (66.6–96.2)	69.6 (62.0–82.7)	0.19
Peel lung				
80% peel lung	47.9 (39.3–58.5)	48.3 (40.5–62.3)	45.8 (35.9–53.0)	0.24
50% peel lung	14.4 (11.0–19.3)	14.5 (11.6–25.0)	12.6 (9.5–18.4)	0.23
20% peel lung	2.0 (1.2–3.3)	2.1 (1.2–3.8)	1.9 (1.0–2.9)	0.38
Core lung				
80% core lung	72.2 (62.8–90.0)	73.4 (63.7–91.4)	68.0 (60.6–79.6)	0.22
50% core lung	59.8 (50.5–72.8)	61.2 (50.2–73.7)	53.9 (50.7–64.7)	0.29
20% core lung	27.1 (23.8–32.5)	27.2 (24.4–33.1)	25.8 (21.7–29.7)	0.40

Median vessel volumes corrected for body surface area are given in mL/m² with interquartile range in parentheses. PH, pulmonary hypertension.

to the patients' records, whereas 4/48 patients (8.3%) had been classified as group 2 PH according to previous definitions, despite having a PAWP <15 mmHg at rest. Finally, 4/48 patients (8.3%) had previously been classified as borderline PH and were classified as having precapillary PH according to the updated hemodynamic definition.

Intrapulmonary vessel volumes

Median total lung volume of the study cohort based on automated lung segmentation was 4,792.1 mL (IQR, 4,079.8–5,786.4 mL). Median lung volumes did not differ significantly between patients with postcapillary PH (4,548.9 mL, IQR, 3,974.6–5,019.7 mL) and precapillary PH (4,976.1 mL, IQR, 4,120.2–6,182.8 mL, $P=0.07$). Median whole lung intrapulmonary vessel volumes were 74.1 mL/m² (IQR, 64.8–91.9 mL/m²) in all included patients, 69.6 mL/m² (IQR, 62.0–82.7 mL/m²) in patients with postcapillary PH and 75.0 mL/m² (IQR, 66.6–96.2 mL/m², $P=0.19$) in patients with precapillary PH (Table 2, Figures 3,4).

Correlation of intrapulmonary vessel volumes with pulmonary hemodynamics in patients with postcapillary PH

Correlation coefficients of intrapulmonary vascular volumes and RHC measurements in patients with postcapillary PH are summarised in Figure 3B and Table S1. A strong positive correlation was found between 50% core vessel volume and mPAP ($r=0.71$, 95% CI: 0.38, 0.90, $P<0.001$), which

was also the strongest correlation observed overall between intrapulmonary vessel volumes and RHC measurements. Correlations with mPAP of 80% core lung vessel volume ($r=0.57$, 95% CI: 0.15, 0.86, $P=0.003$), 20% core lung vessel volume ($r=0.58$, 95% CI: 0.16, 0.86, $P=0.003$) and total intrapulmonary vessel volume ($r=0.58$, 95% CI: 0.14, 0.87, $P=0.003$) were moderate.

Correlations between peel vessel volumes and mPAP increased with increasing peel size from negligible ($r=0.05$, $P=0.82$ for 20% peel lung volume) to moderate at 80% peel lung volume ($r=0.54$, 95% CI: 0.09, 0.85, $P=0.007$).

Correlations with PAWP were weakly to moderately positive with a maximum at 80% core lung volume ($r=0.40$, 95% CI: -0.05, 0.75, $P=0.05$).

Correlations with PVR were negligible to moderate with a maximum at 50% core lung volume ($r=0.45$, 95% CI: 0.05, 0.74, $P=0.03$).

Correlations were also analysed in the subgroup of patients with combined pre- and postcapillary PH and correlations with mPAP were slightly stronger. Especially, vessel volume in 50% core lung volume correlated even more strongly with mPAP ($r=0.76$, 95% CI: 0.47, 0.94, $P<0.001$). Correlations with PAWP were slightly weaker, for example 80% core lung vessel volume ($r=0.32$, $P=0.18$). Correlation with PVR was slightly stronger and showed moderate correlation with core vessel volumes, for example 50% core lung volume ($r=0.51$, $P=0.02$).

Analyses were also conducted without prior correction for each patient's BSA; however, correlations were generally weaker without BSA-correction. For example, correlation of

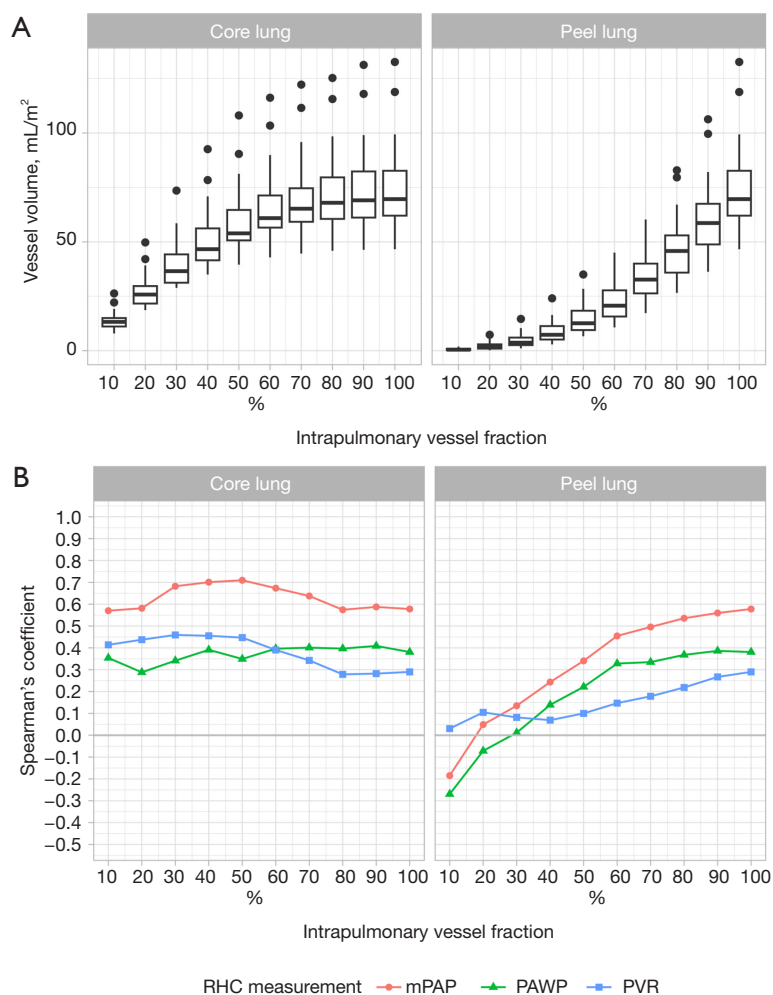


Figure 3 Correlation of intrapulmonary vessel volume fractions with right heart catheter measurements in patients with postcapillary pulmonary hypertension. Intrapulmonary vessel volumes corrected for body surface area (A) within varying core (A, left) and peel (A, right) fractions of the lung volume in patients with postcapillary pulmonary hypertension are shown along with the corresponding Spearman's correlation coefficients (B) with RHC measurements mPAP, PAWP and PVR. RHC, right heart catheter; mPAP, mean pulmonary arterial pressure; PAWP, pulmonary arterial wedge pressure; PVR, pulmonary vascular resistance.

vessel volume within 50% core lung volume without BSA-correction with mPAP was $r=0.56$ ($P=0.004$).

Influence of possible confounders on non-invasive estimation of mPAP in patients with postcapillary PH was analysed by means of multivariable linear regression analysis (Table 3). Age and sex in addition to 50% core lung vessel volume were included in the analysis. However, age and sex did not significantly contribute to the resulting regression models and inclusion of either or both of the additional parameters did not result in improved adjusted r^2 of the model.

Correlation of intrapulmonary vessel volumes with pulmonary hemodynamics in patients with precapillary PH

In patients with precapillary PH, only negligible or weak correlations were found with mPAP (80% peel lung $r=-0.13$, $P=0.37$), PAWP (20% peel lung $r=-0.24$, $P=0.10$) and PVR (50% core lung $r=-0.09$, $P=0.53$, Figure 4B, Table S1).

Correlation coefficients for all included patients in the study cohort were negligible or weak for mPAP, (20% core lung $r=0.14$, $P=0.23$), PAWP (20% peel lung $r=-0.20$, $P=0.10$) and PVR (20% core lung $r=0.15$, $P=0.22$, Table S1).

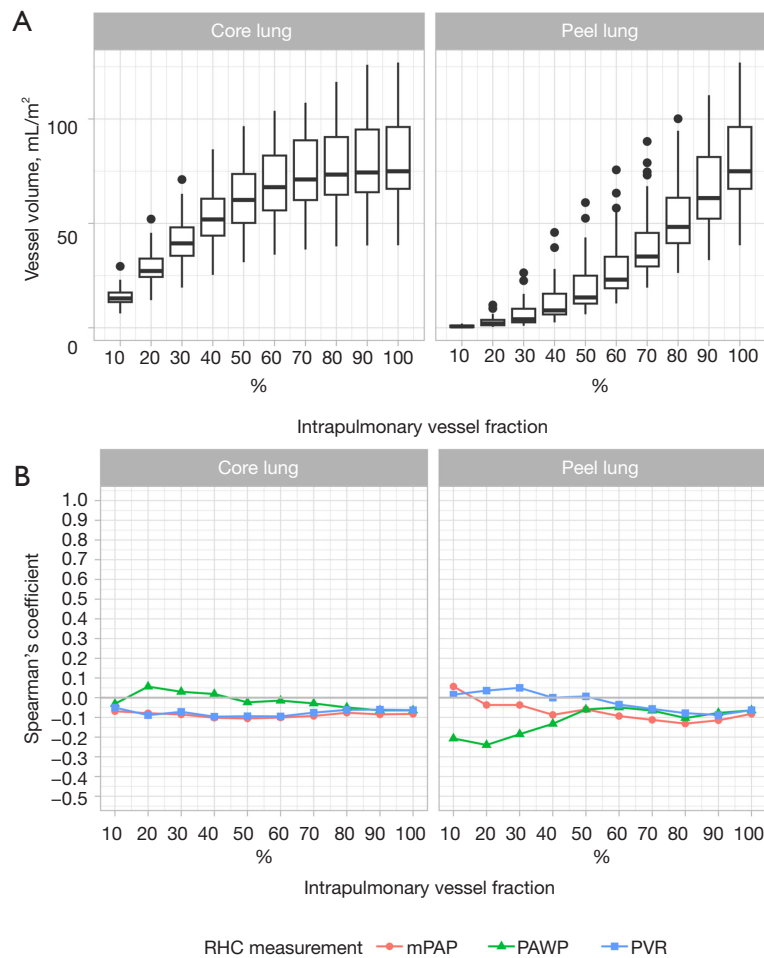


Figure 4 Correlation of intrapulmonary vessel volume fractions with right heart catheter measurements in patients with precapillary pulmonary hypertension. Intrapulmonary vessel volumes corrected for body surface area (A) within varying core (A, left) and peel (A, right) fractions of the lung volume in patients with precapillary pulmonary hypertension are shown along with the corresponding Spearman's correlation coefficients (B) with RHC measurements mPAP, PAWP and PVR. RHC, right heart catheter; mPAP, mean pulmonary arterial pressure; PAWP, pulmonary arterial wedge pressure; PVR, pulmonary vascular resistance.

Influence of CO and PH group on intrapulmonary core vessel volume

A linear regression analysis was conducted to assess the potential influence of CO or PH group besides mPAP on measured intrapulmonary vessel volume within 50% core lung volume. Only patients with PH groups 1, 2 or 4 were included due to the small number of only 5 patients with PH group 3. Neither PH group nor CO significantly contributed to the explanation of intrapulmonary vascular volume or improved model fit (Table S2). mPAP was the only significant predictor of intrapulmonary vessel volume of the chosen variables.

Discussion

Key findings

We conducted a systematic analysis of automated volumetry of intrapulmonary vasculature within varying core and peel fractions of the lung volume in patients with post- and precapillary PH, according to the updated 2022 ESC/ERS guidelines on PH (1). In patients with postcapillary PH, strong correlations of vessel volumes in the core lung with mPAP and weak to moderate correlations with PAWP and PVR were observed. The strongest correlation was observed between the intrapulmonary vessel volume within 50% core lung volume and mPAP with a correlation

Table 3 Multivariable linear regression analysis of BSA-corrected intrapulmonary vascular volume within 50% lung core volume and age and sex as potential confounders for the prediction of mPAP in patients with postcapillary PH

Models	Variables	Estimate	Standard error	Standardized beta coefficient	P value	Adjusted r ²
Model 1	Intercept	-0.768	18.131	-	0.97	0.424
	50% core lung vessel volume	0.510	0.1152	0.748	<0.001	
	Age	0.100	0.195	0.083	0.61	
	Sex	4.460	4.730	0.159	0.36	
Model 2	Intercept	7.385	8.684	-	0.40	0.444
	50% core lung vessel volume	0.500	0.112	0.733	<0.001	
	Age	-	-	-	-	
	Sex	4.073	4.588	0.145	0.38	
Model 3	Intercept	6.983	16.117	-	0.67	0.423
	50% core lung vessel volume	0.475	0.109	0.696	<0.001	
	Age	0.071	0.192	0.059	0.71	
	Sex	-	-	-	-	
Model 4	Intercept	12.426	6.539	-	0.07	0.449
	50% core lung vessel volume	0.469	0.106	-	<0.001	
	Age	-	-	-	-	
	Sex	-	-	-	-	

Model 1: full model including 50% core lung vessel volume as well as age and sex as potential confounders for the prediction of mPAP. Model 2: only sex is included as a potential confounder. Model 3: only age is included as a potential confounder. Model 4: univariate regression analysis of 50% core lung vessel volume for the prediction of mPAP. BSA, body surface area; mPAP, mean pulmonary arterial pressure; PH, pulmonary hypertension.

coefficient of 0.71. Age and sex did not significantly affect this correlation.

Strengths and limitations

A strength of this study is the systematic analysis of intrapulmonary vessel volumes in concentric core and peel fractions of the lung volume, which, to our knowledge, has not been previously published. Furthermore, we conducted the analysis in a group of patients with PH status defined according to the most recent hemodynamic definition and correlated derived vessel volumes with RHC measurements, which is the gold-standard for the assessment of pulmonary hemodynamics. However, several limitations of this study have to be considered. We conducted a retrospective analysis in a small number of patients at a single PH centre, therefore validation of the findings in a larger, prospective study is desirable. Furthermore, our methodology is limited

to the analysis of combined arterial and venous vessel volumes.

Comparison with similar researches

Previous studies on changes in the intrapulmonary vasculature in patients with PH have focused on CT correlates of “vascular pruning” as observed on angiography or radiography and correspondingly loss of small vessels with <5 mm² cross-sectional area (17,20,21,30). A study by Matsuoka and colleagues also investigated larger intrapulmonary vessels with 5–10 mm² cross-sectional area in patients with severe emphysema but did not find a significant correlation between their total cross-sectional area and mPAP (30). A recent study by Shahin *et al.* also investigated CTPA-based volume of vessels up to 2 mm in diameter and total volume of pulmonary arteries and veins within peels of 15, 30, and 45 mm from the lung surface

in a large cohort of patients with different subtypes of PH and patient controls (23). They reported weak negative correlations between small vessel volume and PAWP with correlation coefficients of $r=-0.10$ to -0.19 but no evidence of correlation between small vessel volume and mPAP (23). This is similar to our findings in patients with precapillary PH, in which we found weak, non-significant negative correlation of -0.26 between PAWP and 10% peel lung vessel volume and negligible correlation of intrapulmonary vessel volumes with mPAP.

Explanations of findings

Postcapillary PH, both isolated as well as combined pre- and postcapillary PH, is mainly the result of left heart disease (PH group 2) and represents the most common form of PH overall (1). In addition to increases in diameter or volume of the main pulmonary arteries, as demonstrated for PH in general (7-12), an enlargement of the left atrium has been identified as a distinctive feature of patients with postcapillary PH on cross-sectional imaging (13,16,31,32). Enlargement of central intrapulmonary veins in the upper lobes on upright anteroposterior chest radiographs is a well-known, semi-quantitative measure of pulmonary congestion (33-35). On supine cross-sectional imaging, enlargement and increased tortuosity of central pulmonary veins have also been acknowledged as potential qualitative findings of postcapillary PH on CT (36). However, there is a lack of quantitative measurements concerning the intrapulmonary vasculature in patients with postcapillary PH. A recent study of 232 patients investigated several qualitative imaging features of acute heart failure on unenhanced CT scans of the chest and found increased vessel diameters to be a significant imaging biomarker of acute heart failure with an odds ratio of 4.49 (37). Furthermore, the four central pulmonary veins are known to be dilated in patients with atrial fibrillation and this has been shown to be reversible after catheter ablation (38-40). The association between intrapulmonary vessel volume in the core lung and mPAP in patients with postcapillary PH observed in our study may, therefore, be expected and likely reflects a combined dilation of pulmonary veins and arteries in the core lung in these patients. This may be supported by the finding of an even stronger correlation in the subgroup of patients with combined pre- and postcapillary PH. On the other hand, correlations with PAWP in postcapillary PH patients were only moderate, even in the core lung, although this parameter differentially defines postcapillary PH. We

again believe this may potentially be explained by the lack of differentiation between arterial and venous vessels with our method and such variations may be obscured by overall variability in pulmonary vessel volume. Furthermore, pulmonary venous vessel volume may also be more prone to short term variations in pulmonary venous pressure, that may have occurred during the interval between RHC and CT examination.

Implications and actions needed

The presented technique has potential to aid in non-invasive estimation of pulmonary hemodynamics in patients with postcapillary PH who undergo CTPA and may thereby assist decision-making for invasive RHC assessment and treatment. However, the findings require validation in larger, prospective studies. Also, further exploration of the technique as a non-invasive treatment monitoring tool in serial examinations is desirable.

Conclusions

Automated segmentation of intrapulmonary vasculature on CTPA revealed strong correlations between intrapulmonary vessel volumes in the core lung and invasively measured mPAP in patients with postcapillary PH according to the updated 2022 ESC/ERS guidelines on PH. We identified 50% core lung volume as the lung fraction with the strongest correlation between vessel volume and mPAP. If confirmed in future studies, the technique might improve non-invasive estimation of pulmonary hemodynamics in patients with postcapillary PH undergoing CTPA, and may have further potential for therapeutic monitoring.

Acknowledgments

Funding: This study was supported by the German Center for Lung Research (DZL) through grants from the German Ministry for Education and Science (BMBF; 82DZL00401, 82DZL00402, 82DZL00404).

Footnote

Reporting Checklist: The authors have completed the STROBE reporting checklist. Available at <https://cdt.amegroups.com/article/view/10.21037/cdt-24-293/rc>

Data Sharing Statement: Available at <https://cdt.amegroups.com>

[com/article/view/10.21037/cdt-24-293/dss](https://doi.org/10.21037/cdt-24-293/dss)

Peer Review File: Available at <https://cdt.amegroups.com/article/view/10.21037/cdt-24-293/prf>

Conflicts of Interest: All authors have completed the ICMJE uniform disclosure form (available at <https://cdt.amegroups.com/article/view/10.21037/cdt-24-293/coif>). M.O.W. reports that he has received study grants from Vertex Pharmaceuticals, paid to institutions; consulting fees from Vertex Pharmaceuticals and Boehringer Ingelheim, paid to institution and honoraria for lectures etc. from Vertex Pharmaceuticals, paid to institution. E.G. reports that he has received research grants outside the submitted work by Accelerant, Actelion, Janssen, Bayer, MSD, Ferrer, Merck, Liquidia, UT, OMT paid to the institution; consulting fees by Actelion, Janssen, Bayer, MSD, Merck, Ferrer outside the submitted work paid to him; speaker honoraria outside the submitted work by Actelion, Bayer, MSD, GSK, AOP, Janssen, ph ev, OMT, GEBRO, Ferrer, GWT paid to him and that he is a member of the ADue Steering committee, paid outside the submitted work and an unpaid scientific advisory board member of ph eV. H.U.K. reports that he received grants from Siemens, Philips, Boehringer Ingelheim paid to the institution and honoraria for speaking or advisory board participation from Siemens, Philips, Boehringer Ingelheim, Median, contextflow, paid to him. For Claus Peter Heussel's potential COI, see his COI statement at <https://cdt.amegroups.com/article/view/10.21037/cdt-24-293/coif>. F.R. reports that he is, at the time of submission, an employee of Bayer AG, Germany, but the work presented herein dates to his previous employment at Heidelberg University Hospital. The other authors have no conflicts of interest to declare.

Ethical Statement: The authors are accountable for all aspects of the work in ensuring that questions related to the accuracy or integrity of any part of the work are appropriately investigated and resolved. The study was conducted in accordance with the Declaration of Helsinki (as revised in 2013). The study was approved by the ethics committee of the medical faculty of Heidelberg University (No. S-592/2016) and individual consent for this retrospective analysis was waived.

Open Access Statement: This is an Open Access article distributed in accordance with the Creative Commons Attribution-NonCommercial-NoDerivs 4.0 International

License (CC BY-NC-ND 4.0), which permits the non-commercial replication and distribution of the article with the strict proviso that no changes or edits are made and the original work is properly cited (including links to both the formal publication through the relevant DOI and the license). See: <https://creativecommons.org/licenses/by-nc-nd/4.0/>.

References

- Humbert M, Kovacs G, Hoeper MM, et al. 2022 ESC/ERS Guidelines for the diagnosis and treatment of pulmonary hypertension. *Eur Heart J* 2022;43:3618-731.
- Galiè N, Humbert M, Vachiery JL, et al. 2015 ESC/ERS Guidelines for the diagnosis and treatment of pulmonary hypertension: The Joint Task Force for the Diagnosis and Treatment of Pulmonary Hypertension of the European Society of Cardiology (ESC) and the European Respiratory Society (ERS): Endorsed by: Association for European Paediatric and Congenital Cardiology (AEPC), International Society for Heart and Lung Transplantation (ISHLT). *Eur Heart J* 2016;37:67-119.
- Simonneau G, Montani D, Celermajer DS, et al. Haemodynamic definitions and updated clinical classification of pulmonary hypertension. *Eur Respir J* 2019;53:1801913.
- Hoeper MM, Humbert M, Souza R, et al. A global view of pulmonary hypertension. *Lancet Respir Med* 2016;4:306-22.
- Tuder RM, Marecki JC, Richter A, et al. Pathology of pulmonary hypertension. *Clin Chest Med* 2007;28:23-42, vii.
- Gray HH, Morgan JM, Kerr IH, et al. Clinical correlates of angiographically diagnosed idiopathic pulmonary hypertension. *Thorax* 1990;45:442-6.
- Kuriyama K, Gamsu G, Stern RG, et al. CT-determined pulmonary artery diameters in predicting pulmonary hypertension. *Invest Radiol* 1984;19:16-22.
- Shen Y, Wan C, Tian P, et al. CT-base pulmonary artery measurement in the detection of pulmonary hypertension: a meta-analysis and systematic review. *Medicine (Baltimore)* 2014;93:e256.
- Truong QA, Massaro JM, Rogers IS, et al. Reference values for normal pulmonary artery dimensions by noncontrast cardiac computed tomography: the Framingham Heart Study. *Circ Cardiovasc Imaging* 2012;5:147-54.
- Froelich JJ, Koenig H, Knaak L, et al. Relationship between pulmonary artery volumes at computed tomography and pulmonary artery pressures in patients with- and without pulmonary hypertension. *Eur J Radiol*

- 2008;67:466-71.
11. Rengier F, Wörz S, Melzig C, et al. Automated 3D Volumetry of the Pulmonary Arteries based on Magnetic Resonance Angiography Has Potential for Predicting Pulmonary Hypertension. *PLoS One* 2016;11:e0162516.
 12. Melzig C, Wörz S, Egenlauf B, et al. Combined automated 3D volumetry by pulmonary CT angiography and echocardiography for detection of pulmonary hypertension. *Eur Radiol* 2019;29:6059-68.
 13. Aviram G, Rozenbaum Z, Ziv-Baran T, et al. Identification of Pulmonary Hypertension Caused by Left-Sided Heart Disease (World Health Organization Group 2) Based on Cardiac Chamber Volumes Derived From Chest CT Imaging. *Chest* 2017;152:792-9.
 14. Aviram G, Shmueli H, Adam SZ, et al. Pulmonary Hypertension: A Nomogram Based on CT Pulmonary Angiographic Data for Prediction in Patients without Pulmonary Embolism. *Radiology* 2015;277:236-46.
 15. Melzig C, Do TD, Egenlauf B, et al. Utility of Automated Cardiac Chamber Volumetry by Nongated CT Pulmonary Angiography for Detection of Pulmonary Hypertension Using the 2018 Updated Hemodynamic Definition. *AJR Am J Roentgenol* 2022;219:66-75.
 16. Melzig C, Do TD, Egenlauf B, et al. Diagnostic accuracy of automated 3D volumetry of cardiac chambers by CT pulmonary angiography for identification of pulmonary hypertension due to left heart disease. *Eur Radiol* 2022;32:5222-32.
 17. Rahaghi FN, Ross JC, Agarwal M, et al. Pulmonary vascular morphology as an imaging biomarker in chronic thromboembolic pulmonary hypertension. *Pulm Circ* 2016;6:70-81.
 18. Goo HW, Park SH. Prediction of pulmonary hypertension using central-to-peripheral pulmonary vascular volume ratio on three-dimensional cardiothoracic CT in patients with congenital heart disease. *Jpn J Radiol* 2022;40:961-9.
 19. Goo HW, Park SH. Pulmonary vascular volume ratio measured by cardiac computed tomography in children and young adults with congenital heart disease: comparison with lung perfusion scintigraphy. *Pediatr Radiol* 2017;47:1580-7.
 20. Synn AJ, Li W, San José Estépar R, et al. Pulmonary Vascular Pruning on Computed Tomography and Risk of Death in the Framingham Heart Study. *Am J Respir Crit Care Med* 2021;203:251-4.
 21. Synn AJ, Margerie-Mellon C, Jeong SY, et al. Vascular remodeling of the small pulmonary arteries and measures of vascular pruning on computed tomography. *Pulm Circ* 2021;11:20458940211061284.
 22. Estépar RS, Kinney GL, Black-Shinn JL, et al. Computed tomographic measures of pulmonary vascular morphology in smokers and their clinical implications. *Am J Respir Crit Care Med* 2013;188:231-9.
 23. Shahin Y, Alabed S, Alkhanfar D, et al. Quantitative CT Evaluation of Small Pulmonary Vessels Has Functional and Prognostic Value in Pulmonary Hypertension. *Radiology* 2022;305:431-40.
 24. Du Bois D, Du Bois EF. A formula to estimate the approximate surface area if height and weight be known. *Nutrition* 1989;5:303-11; discussion 312-3.
 25. Konietzke P, Weinheimer O, Wielpütz MO, et al. Validation of automated lobe segmentation on paired inspiratory-expiratory chest CT in 8-14 year-old children with cystic fibrosis. *PLoS One* 2018;13:e0194557.
 26. Achenbach T, Weinheimer O, Buschsieweke C, et al. Fully automatic detection and quantification of emphysema on thin section MD-CT of the chest by a new and dedicated software. *Rofo* 2004;176:1409-15.
 27. Do TD, Skornitzke S, Merle U, et al. COVID-19 pneumonia: Prediction of patient outcome by CT-based quantitative lung parenchyma analysis combined with laboratory parameters. *PLoS One* 2022;17:e0271787.
 28. Konietzke P, Brunner C, Konietzke M, et al. GOLD stage-specific phenotyping of emphysema and airway disease using quantitative computed tomography. *Front Med (Lausanne)* 2023;10:1184784.
 29. Overholser BR, Sowinski KM. Biostatistics primer: part 2. *Nutr Clin Pract* 2008;23:76-84.
 30. Matsuoka S, Washko GR, Yamashiro T, et al. Pulmonary hypertension and computed tomography measurement of small pulmonary vessels in severe emphysema. *Am J Respir Crit Care Med* 2010;181:218-25.
 31. Currie BJ, Johns C, Chin M, et al. CT derived left atrial size identifies left heart disease in suspected pulmonary hypertension: Derivation and validation of predictive thresholds. *Int J Cardiol* 2018;260:172-7.
 32. Jivraj K, Bedayat A, Sung YK, et al. Left Atrium Maximal Axial Cross-Sectional Area is a Specific Computed Tomographic Imaging Biomarker of World Health Organization Group 2 Pulmonary Hypertension. *J Thorac Imaging* 2017;32:121-6.
 33. Barile M. Pulmonary Edema: A Pictorial Review of Imaging Manifestations and Current Understanding of Mechanisms of Disease. *Eur J Radiol Open* 2020;7:100274.
 34. Melzig C, Rengier F. Increased pulmonary arterial and venous pressure. *Radiologe* 2022;62:120-9.

35. Porres DV, Morenza OP, Pallisa E, et al. Learning from the pulmonary veins. *Radiographics* 2013;33:999-1022.
36. Tsai IC, Tsai WL, Wang KY, et al. Comprehensive MDCT evaluation of patients with pulmonary hypertension: diagnosing underlying causes with the updated Dana Point 2008 classification. *AJR Am J Roentgenol* 2011;197:W471-81.
37. Miger K, Fabricius-Bjerre A, Overgaard Olesen AS, et al. Chest computed tomography features of heart failure: A prospective observational study in patients with acute dyspnea. *Cardiol J* 2022;29:235-44.
38. Schwartzman D, Lacomis J, Wigginton WG. Characterization of left atrium and distal pulmonary vein morphology using multidimensional computed tomography. *J Am Coll Cardiol* 2003;41:1349-57.
39. Tsao HM, Yu WC, Cheng HC, et al. Pulmonary vein dilation in patients with atrial fibrillation: detection by magnetic resonance imaging. *J Cardiovasc Electrophysiol* 2001;12:809-13.
40. Tsao HM, Wu MH, Huang BH, et al. Morphologic remodeling of pulmonary veins and left atrium after catheter ablation of atrial fibrillation: insight from long-term follow-up of three-dimensional magnetic resonance imaging. *J Cardiovasc Electrophysiol* 2005;16:7-12.

Cite this article as: Melzig C, Weinheimer O, Egenlauf B, Do TD, Wielpütz MO, Grünig E, Kauczor HU, Heussel CP, Rengier F. Automated volumetry of core and peel intrapulmonary vasculature on computed tomography angiography for non-invasive estimation of hemodynamics in patients with pulmonary hypertension (2022 updated hemodynamic definition). *Cardiovasc Diagn Ther* 2024;14(6):1083-1095. doi: 10.21037/cdt-24-293